

# Diffusivities and front propagation in sedimentation<sup>a)</sup>

P. J. Mucha

*School of Mathematics and Center for Dynamical Systems and Nonlinear Studies,  
Georgia Institute of Technology, Atlanta, Georgia 30332-0160*

M. P. Brenner

*Division of Engineering and Applied Sciences, Harvard University, Cambridge, Massachusetts 02139*

(Received 14 June 2002; accepted 24 October 2002; published 4 April 2003)

Continuum models for particles sedimenting in a fluid often assume that the diffusivity is a local function of the particulate volume fraction. Since the hydrodynamically induced diffusivity is a result of the velocity fluctuations of particles, the recent identification [e.g., Tee *et al.*, Phys. Rev. Lett. **89**, 054501 (2002)] of particle density stratification as a controlling parameter for the velocity fluctuations also extends to the diffusivities. In particular, the stratification control strongly affects the diffusivity in the vicinity of the falling sediment front between particle-laden fluid below and clarified fluid above. The resulting scaling for stratification-controlled diffusivities in creeping flow sedimentation is presented and compares favorably with measurements from dilute-limit particle simulations. Steadily falling concentration profiles for dilute sedimentation with these diffusivities are then presented, and an extension of the model to higher volume fractions is discussed. © 2003 American Institute of Physics. [DOI: 10.1063/1.1564824]

## I. INTRODUCTION

While the “microscopic” dynamics of individual solid particles suspended in a fluid are well understood,<sup>1,2</sup> the “macroscopic” properties of flows with large numbers of particles can be exceedingly complicated. The dynamics of particles sedimenting in a highly viscous fluid has received significant attention over the years, including consideration of polydisperse, flocculent, and nonspherical sedimenting particles (see, e.g., the review by Davis and Acrivos<sup>3</sup> and the collections which start with Refs. 4 and 5). Nevertheless, answers to fundamental questions about monodisperse non-flocculent rigid sedimenting spheres have been slow in coming, primarily because of the long-ranged nature of the hydrodynamic interactions between particles at very low Reynolds number.<sup>6–8</sup>

The average rate of settling,  $V$ , and its dependence on particulate volume fraction,  $\phi$ , is well understood in dilute systems,<sup>9,10</sup> and a number of empirical  $V(\phi)$  relationships at higher volume fractions have been tested successfully.<sup>3</sup> Individual particles, however, move with velocities that fluctuate about the mean over time, both in the direction of gravity and in the perpendicular horizontal plane, giving rise to a hydrodynamically induced diffusivity.<sup>11–15</sup> These velocity fluctuations have been the subject of significant controversy focusing on whether or not they are system-size dependent (see, e.g., Refs. 16 and 17, and the review by Ramaswamy<sup>18</sup> and references therein). Nevertheless, macroscopic models of sedimentation<sup>11–13,15,19–23</sup> typically assume that the diffusion coefficient,  $D$ , is a local function solely dependent on particle concentration, i.e.,  $D = D(\phi)$ .

Recent investigations<sup>24</sup> (cf. Refs. 25 and 26) have demonstrated that, in fact, the velocity fluctuations depend on system geometry in subtle ways, both through the system dimensions and through particle concentration gradients. This understanding of the velocity fluctuations calls into question formulas for  $D$  which are solely in terms of volume fraction. The goal of this paper is to propose a simple model for  $D$  and test it on a process where diffusion is important, the evolution of the sediment front between particle-laden fluid below and clarified fluid above.

In a continuum model, the particle concentration profile of a sediment front evolves through the competition of diffusive front spreading and self-sharpening due to hindered settling,<sup>27</sup> described as an advection-diffusion process

$$\frac{\partial \phi}{\partial t} - \frac{\partial}{\partial z} \{ \phi [ V(\phi) - V_{\text{sed}} ] \} = \frac{\partial}{\partial z} \left[ D \frac{\partial \phi}{\partial z} \right], \quad (1)$$

in a frame falling downwards at speed  $V_{\text{sed}}$ , where  $V(\phi) = V_0 H(\phi)$ ,  $V_0 > 0$  is the terminal Stokes velocity of an individual isolated particle,  $H(\phi) > 0$  captures the hindered settling effect, and  $z$  increases moving up against gravity. Our understanding of the velocity fluctuations leads us to propose a model for the diffusivity that depends on *both* concentration and vertical concentration gradient,  $D(\phi, \partial \phi / \partial z)$ , over a wide range of parameters, and determined in part by the system dimensions. Solutions of Eq. (1) can be compared with particle simulations to test this model against the  $D = D(\phi)$  assumption.

This paper is organized as follows. We describe the scaling for stratification control of the diffusion coefficient in Sec. II. In Sec. III, we present diffusivities obtained near the sediment front in dilute-limit simulations of up to 400 000 sedimenting particles between a pair of no-slip side walls, and compare with the scaling from Sec. II. In Sec. IV, we

<sup>a)</sup>This paper was originally presented as part of the Dan Joseph Symposium at USNCTAM14 in Blacksburg, VA on June 25, 2002.

solve Eq. (1), with this diffusivity model, for the steadily falling fronts separating dilute sedimenting particles below from clear fluid above. We then describe an extension of this model to sedimentation at higher volume fractions in Sec. V, followed by concluding remarks in Sec. VI.

## II. THE ROLE OF STRATIFICATION

The seemingly conflicting velocity fluctuations results that have been obtained in experiments, simulations, and theoretical ideas appear to have been resolved recently with the central idea being that the magnitude of velocity fluctuations can be controlled by exceedingly small stable vertical gradients of the particle concentration. Luke<sup>25</sup> demonstrated that stably stratified particle densities can cause the fluctuations to decrease at short times below those predicted by an independent Poisson distribution, and recent simulations<sup>26</sup> have verified that the presence of a container bottom is important in decreasing velocity fluctuations. Although we agree with Luke's description of the short-time decay of fluctuations, we disagree with the assertion that this decay persists in a locally constant stratification; rather, the velocity fluctuations relax to values which are smaller than those of an independent Poisson distribution and remain statistically steady at long times in a locally constant density stratification.<sup>24</sup> Below some "critical" stratification, the fluctuations are set by the cell size; above the critical stratification, the fluctuations decrease with increasing local stratification. The fact that the critical stratification between these two regimes becomes arbitrarily small as the system size increases is obtained as a direct consequence of the theoretical argument outlined below, so that many physical systems are in the stratification-controlled regime despite the self-sharpening of the front due to hindered settling.<sup>28</sup>

Velocity fluctuations are driven by fluctuations in particle concentration. Under Poisson number density fluctuations, a region of size  $\ell$  has a typical concentration fluctuation of  $\Delta\phi \approx \sqrt{\phi a^3/\ell^3}$ . The velocity of this region in a fluid of viscosity  $\eta$  is determined by balancing its buoyant weight,  $g\ell^3\Delta\phi\Delta\rho \sim \ell^3\Delta\phi(\eta V_0/a^2)$ , with its Stokes drag,  $\approx 6\pi\eta\ell\Delta V$ , giving  $\Delta V \sim V_0\sqrt{\phi\ell/a}$ . The largest  $\Delta V$  fluctuations are then obtained by the largest such regions in the system, the determination of which is dominated by the smallest dimension of the container holding the sediment,<sup>29</sup>  $\ell \sim d$ , giving  $\Delta V \sim V_0\sqrt{\phi d/a}$ . This physical argument<sup>17</sup> reproduces the same scaling obtained from Poisson averages by Caffisch and Luke.<sup>16</sup> These Poisson concentration fluctuations at a scale  $\ell$  are produced and destroyed due to randomness on the same time scale,  $\ell/\Delta V$ ; thus they are advected a distance  $\sim \ell$  in their lifetime, and create an effective diffusivity,  $D \sim \ell\Delta V \sim V_0\sqrt{\phi d^3/a}$ .

The presence of a stable macroscopic particle density gradient changes the above picture. If the change in concentration due to stratification is greater than the  $\Delta\phi$  fluctuations at some length scale, the buoyancy mismatch is lost, the fluctuations at that scale can no longer advect as far, and the suppression of this motion further suppresses density fluctuations at that scale. For a locally linear decrease in  $\phi$  with height,  $\phi = \phi_0(1 - \beta z)$ ,  $\beta > 0$ , the change in concentration

due to stratification at a scale  $\ell$  is the same as the  $\Delta\phi$  fluctuations when  $\beta\phi\ell \sim \sqrt{\phi a^3/\ell^3}$ . Since the effect of stratification increases with size, the largest fluctuations not suppressed by stratification then scale like

$$\ell \sim a\phi^{-1/5}(\beta a)^{-2/5} \sim a\phi^{1/5} \left| a \frac{\partial\phi}{\partial z} \right|^{-2/5}. \quad (2)$$

This scale is smaller than that set by the container size provided  $\beta$  is larger than some "critical" value which would give  $\ell \sim d$ ,  $\beta_{\text{crit}} \sim [d\sqrt{\phi(d/a)^3}]^{-1}$ . At  $\beta > \beta_{\text{crit}}$ , the fluctuations controlled by stratification then have velocities

$$\Delta V \sim V_0\phi^{2/5}(\beta a)^{-1/5} \sim V_0\phi^{3/5} \left| a \frac{\partial\phi}{\partial z} \right|^{-1/5}, \quad (3)$$

and create an effective diffusivity

$$D \sim \ell\Delta V \sim aV_0\phi^{1/5}(\beta a)^{-3/5} \sim aV_0\phi^{4/5} \left| a \frac{\partial\phi}{\partial z} \right|^{-3/5}. \quad (4)$$

The above arguments in terms of number density fluctuations reproduce the same scalings as a related argument in terms of time scales,<sup>24</sup> both of which are in agreement with a model computation in terms of the structure factor.<sup>28</sup>

We now proceed to test whether the diffusivities measured from particle simulations agree with the proposed dependence on particle concentration gradient in Eq. (4).

## III. DILUTE-LIMIT SIMULATIONS

The evolution of the sediment front was investigated with simulations of dilute-limit "point-force" interacting particles sedimenting between a pair of no-slip side walls. Similar simulations were used previously<sup>24</sup> to investigate velocity fluctuations. The particle advection interactions are determined by the point-force incompressible Stokes equations, with no-slip side walls separated by a distance  $d$  in the  $x$  direction, and periodic boundary conditions in the  $y$  and  $z$  directions (with periodic lengths  $w$  and  $h$ , respectively,  $d \ll w, h$ ). The fluid velocities generated by a single particle can then be manipulated in a two-dimensional Fourier series representation, and organization of terms into "source" and "response" coefficients leads to an  $O(N \ln N)$  algorithm for calculating the interactions between  $N$  particles. The top and bottom surfaces of the cells are approximated by free-slip, no normal flow surfaces, obtained by including simple images of the sedimenting particles, which is a good approximation at distances  $> d$  from these surfaces. The typical simulations presented here were initiated with particles uniformly distributed in the  $d \times w \times h$  cell up to some maximum height at least  $d$  below the top surface. This restriction was made to minimize the hydrodynamic interaction of the particles with the top surface, so that the primary effect of the cell boundaries in the vertical direction on the development of the falling front is that of a simple barrier which prevents the passage of particles.

The horizontal mixing in the simulations considered here leads to observed particle concentrations that are essentially constant across the horizontal plane, so that we will only concern ourselves with the evolution of the particle concentration as a function of height and time,  $\phi(z, t)$ . The compe-

tion between diffusive spreading and self-sharpening typically complicates the accurate determination of the diffusivity from experimental concentration data, with further complications due to the inherent polydispersity of experimental systems adding an additional front spreading mechanism.<sup>12,19–22</sup> These complications are avoided in the present simulations because there is no hindered settling in the dilute limit of point particles [ $H(\phi) = 1, V(\phi) = V_0$ ], and because the polydispersity inherent in a real experiment is absent in our idealized monodisperse simulations. Under these conditions, the advection-diffusion model, Eq. (1), in the frame falling at the Stokes velocity becomes

$$\frac{\partial \phi}{\partial t} = \frac{\partial}{\partial z} \left[ D \frac{\partial \phi}{\partial z} \right]. \quad (5)$$

Assuming Eq. (5) to be the correct macroscopic model equation for the simulated sediment in the frame falling at  $V_0$ , the diffusivity at a specified point in space and time,  $D(z, t)$ , is obtained after integration over  $z$ , ignoring the effects of the vertical boundaries. The diffusivity is then given by

$$D(z, t) = - \left( \frac{\partial \phi}{\partial z} \right)^{-1} \int_z^\infty dz' \frac{\partial \phi}{\partial t}, \quad (6)$$

assuming  $\phi \rightarrow 0$  as  $z \rightarrow \infty$  (i.e., that there is a sediment front). We use Eq. (6) to measure  $D$  from the particle simulations, computing  $\partial \phi / \partial z$  from smoothed particle concentrations that are averages (convolutions) of the microscopic particle positions with Gaussian envelopes in space. Since the typical correlation length (“swirl size”) of the particle motion is at or slightly below the side wall separation  $d$ , we consider variations in  $\phi$  over lengths larger than this scale, and the standard deviations,  $\sigma$ , of these envelopes are typically a significant fraction of  $d$ . The results shown below do not significantly depend on  $\sigma$ .

A series of simulations were performed in  $8d = w = h$  cells (using  $32 \times 32$  modes in the Fourier series representation of the velocity fields) with particles initially uniformly distributed with concentration  $\phi_0$  in the lower 7/8 of the cell. Vertical particle positions in the falling frame at each time were separated into 10 000 bins, with smoothed concentrations obtained by convolution with Gaussian envelopes. The diffusivities were then calculated by approximating the derivatives in Eq. (6) by centered finite differences. The resulting diffusivities,  $D$ , in the region of the front, are plotted in Fig. 1 versus the local smoothed particle concentration,  $\phi$ , for a series of simulations with 400 000 particles sedimenting under seven different conditions (cell size,  $d/a$ , and initial concentration,  $\phi_0$ ). The specific values of  $D$  vary slightly with the details of this procedure; but the qualitative properties of the figure are insensitive to these details. In particular, the effective separation of the data into a different  $D$  vs  $\phi$  curve for each simulation condition persists across the range of parameters considered for the measurement of the diffusivities.

One might propose that the diffusivities in Fig. 1 should instead give  $D/(aV_0)$  as a function of  $\phi(d/a)^3$ , the relationship that would be expected for velocity fluctuations which

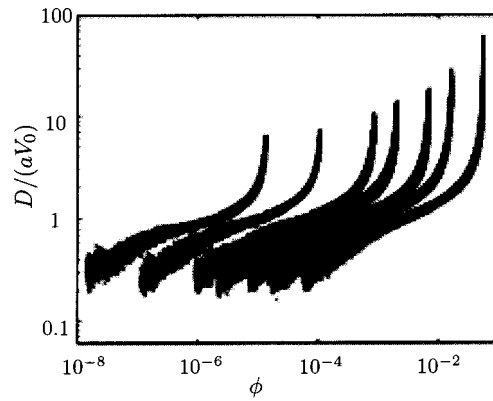


FIG. 1. Diffusivities  $D$  in the region of the front, measured at single instantaneous times via Eq. (6), vs local concentration  $\phi$ , from a series of simulations of 400 000 particles with dilute-limit interactions sedimenting in cells of seven different sizes ( $d/a = 80, 120, 160, 240, 320, 640, 1280$ ). The data, plotted here as a collection of overlapping symbols resulting in the dark regions of the figure, were obtained by smoothing concentrations with Gaussian envelopes of  $\sigma = 0.32d$ , and span concentrations between  $10^{-3} < \phi / \phi_0 < 0.95$  where  $\phi_0$  is the initial concentration in the bulk.

are exclusively controlled by the cell size. Under this hypothesis, the nearly vertical asymptotes at  $\phi = \phi_0$  of the seven separate conditions considered in Fig. 1 align, since  $\phi_0(d/a)^3$  is directly related to the number of particles in the simulation (at fixed cell aspect ratio). Nevertheless, since the seven separate blocks of data in Fig. 1 are not simple horizontal shifts of one another, the collapse of the data for these seven conditions is not particularly good. More importantly, data from simulations with different numbers of particles remain completely separated on such a plot, particularly near the  $\phi = \phi_0$  asymptotes. Even if these nearly vertical asymptotes on such plots could be aligned, the extremely sensitive dependence on  $\phi$  that they would indicate would be problematic; the fact that this alignment cannot be achieved from the simulations under independently varying  $\phi_0$  and  $d/a$  is a direct indication that the diffusivity must be functionally dependent on additional quantities.

The same diffusivities from the region of the evolving front that were plotted in Fig. 1 versus  $\phi$  are replotted in Fig. 2 versus  $\phi^{4/5} [-a(\partial \phi / \partial z)]^{-3/5}$ , with good collapse of the data, usually to within a factor of two (with no averaging except the Gaussian envelope averaging to smooth the particle concentration), while the calculated  $D$ 's vary over two orders of magnitude. This range in  $D \sim \ell \Delta V$  is consistent with velocity fluctuation decays in similar simulations, where  $\Delta V \sim \sqrt{\ell}$  decreases over time from the Poisson predicted values by a factor of 5–8. The apparent noise in the data of Fig. 2 is particularly pronounced near the left edge, corresponding to the very small particle concentrations where the concentration smoothing operation is more sensitive to density fluctuations, and also near the right edge, corresponding to particle concentrations very close to the bulk concentration  $\phi_0$  where the uncertainty in the measurement of the small  $\partial \phi / \partial z$  dominates. This collapse appears to hold across a wide range of independent values of  $\phi_0$  and  $d/a$ , as indicated in Fig. 3, which includes data from 30 different combinations of  $\phi_0$  and  $d/a$  from simulations of

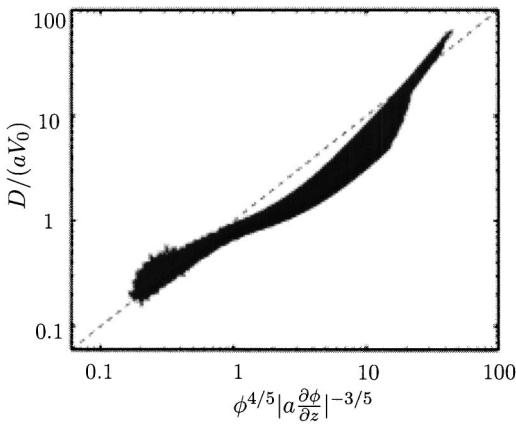


FIG. 2. The same measured diffusivities  $D$  in Fig. 1 vs the product of local concentration  $\phi$  and local stratification of concentration  $\partial\phi/\partial z$  predicted by the stratification scaling of velocity fluctuations, Eq. (4), from a series of simulations of 400 000 particles with dilute-limit interactions sedimenting in cells of seven different sizes. The data plotted here come from measurements of single simulation time frames, resulting in a large number of overlapping symbols which appear as the dark region of the figure. The dashed line,  $D/(aV_0) = \phi^{4/5} |a(\partial\phi/\partial z)|^{-3/5}$ , is given as a reference.

between 5000 and 400 000 particles. The smaller numbers of particles considered as part of Fig. 3 leads to even greater noise in the resulting plot; yet the near collapse of the data is striking when compared with Fig. 1, demonstrating the importance of  $\partial\phi/\partial z$  in determining the size of the diffusion coefficient. Because of the direct connections between the advection-diffusion equations and stochastic models for sedimentation,<sup>30</sup> the identification of  $\partial\phi/\partial z$  as a controlling parameter must also carry over to the parameters of a stochastic model.

The predicted scaling  $D = aV_0 \phi^{4/5} [-a(\partial\phi/\partial z)]^{-3/5}$  from Eq. (4) is included in Figs. 2 and 3 as a reference line.

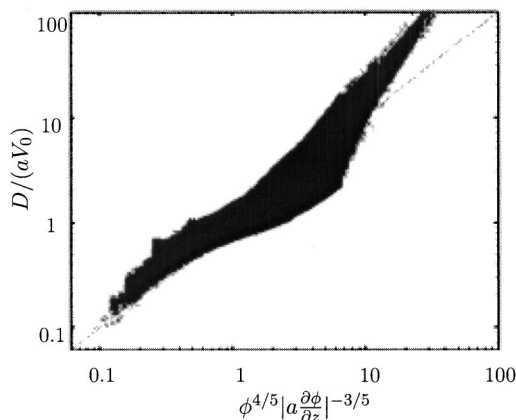


FIG. 3. Diffusivities  $D$  measured via Eq. (6) vs the product of local concentration  $\phi$  and local stratification of concentration  $\partial\phi/\partial z$  predicted by the stratification scaling of velocity fluctuations, Eq. (4), from a series of simulations under 30 different conditions, including simulations of between  $N = 5000$  and 400 000 particles ( $N = 5000$ :  $d/a = 5, 10, 20, 40, 80$ ;  $N = 10\,000$ :  $d/a = 5, 10, 20, 40, 80$ ;  $N = 50\,000$ :  $d/a = 5, 6, 7, 10, 12, 15, 20, 25, 30, 40, 80, 160, 320$ ; and the 7  $d/a$  values at  $N = 400\,000$  plotted previously). The dashed line,  $D/(aV_0) = \phi^{4/5} |a(\partial\phi/\partial z)|^{-3/5}$ , is given as a reference. These data were obtained with Gaussian envelopes of  $\sigma = 0.27d$ , and spans concentrations between  $2.5 \cdot 10^{-3} < \phi/\phi_0 < 0.80$  where  $\phi_0$  is the initial concentration in the bulk.

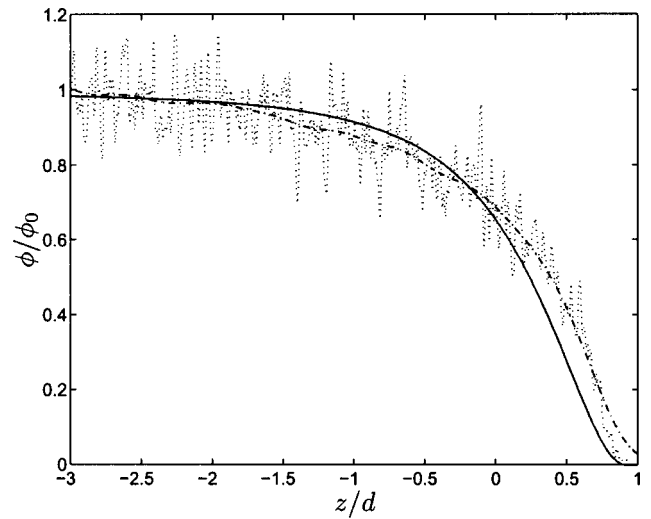


FIG. 4. Comparison of dilute-limit continuum model (solid), defined by Eqs. (5), (7), (8), with observed concentrations  $\phi$  vs height  $z$  from a single frame of a simulation with 50 000 particles. The observed concentrations are Gaussian envelope averages with  $\sigma = 0.0067d$  (dotted) and  $\sigma = 0.167d$  (dashed). The continuum model used here has parameters  $B = 1/2$ ,  $C = 1$  (cf. Figs. 2 and 3).

The data do not precisely collapse onto (or parallel to) the reference line, but this scaling does capture the gross behavior of  $D[\phi, (\partial\phi/\partial z)]$  as measured from the simulations. The remaining spread in the data may be due to finite number effects or may indicate further refinements that could be made to the theory. We proceed by using this simple scaling as a model for the hydrodynamic-induced diffusivity for conditions under which the velocity fluctuations are expected to be controlled by stratification. In particular, we use the model

$$D\left(\phi, \frac{\partial\phi}{\partial z}\right) = \begin{cases} CdV_0\sqrt{\phi d/a} & \text{for } \beta \leq \beta_{\text{crit}} \\ CB^{3/5}aV_0\phi^{4/5} \left| a \frac{\partial\phi}{\partial z} \right|^{-3/5} & \text{for } \beta \geq \beta_{\text{crit}}, \end{cases} \quad (7)$$

where  $\beta \equiv -(1/\phi)(\partial\phi/\partial z)$

$$\beta_{\text{crit}} \equiv B \left[ d \sqrt{\phi \left( \frac{d}{a} \right)^3} \right]^{-1}, \quad (8)$$

and  $B$  and  $C$  are dimensionless constants. Where values of these constants are needed below, we take  $B = 1/2$ , which appears to describe the crossover from cell-size to stratification control of velocity fluctuations in the simulations (we caution that the constant  $B$  has been included in the definition of  $\beta_{\text{crit}}$  here, as opposed to Ref. 24), and  $C = 1$ , which is of the order observed in Figs. 2 and 3.

The resulting dilute-limit model for front evolution given by Eqs. (5), (7), and (8) can be directly compared with the concentrations obtained in the simulations. The observed and predicted concentrations (again, taking  $B = 1/2$  and  $C = 1$ ) for a given single frame typically compare favorably, such as in Fig. 4. Discrepancies are apparent in the figure, indicating imperfections of the model, but this model performs similarly well over a wide range of parameters ( $\phi_0$  and  $d/a$ ) without any changes to the ( $B$ ,  $C$ ) coefficients. In contrast, Fig. 1 demonstrates that restricting the functional

dependence of  $D/(aV_0)$  to volume fraction alone, or to the product  $\phi(d/a)^3$  alone, is insufficient to model the range of conditions considered in the simulations without changing some free parameter. For instance, a given choice of the free parameter  $K$  in  $D = KV_0\sqrt{\phi d^3/a}$  can be selected to give results comparable to those in Fig. 4 for a single set of parameters, but that fitting parameter  $K$  would need to be modified for a different physical condition. Indeed, even a constant-diffusivity  $D = KV_0\sqrt{\phi_0 d^3/a}$  model can give reasonable looking results with a selected  $K \sim O(1)$  for a single or small range of physical conditions;<sup>24</sup> but in such cases  $K$  remains a fitting parameter, whereas the  $(B, C)$  coefficients of the present model appear to remain fixed over wide ranges of the simulation conditions.

#### IV. DILUTE STEADY-STATE PROFILES

We consider the model for the evolution of the concentration defined by Eqs. (1), (7), and (8), with  $V(\phi)/V_0 = 1 - 6.55\phi$  as indicated by Batchelor,<sup>10</sup> and with  $B = 1/2, C = 1$ . The concentration profiles of steadily falling fronts between a bulk concentration  $\phi_0$  below (as  $z \rightarrow -\infty$ ) and  $\phi = 0$  clear fluid above (as  $z \rightarrow \infty$ ) then depend on  $\phi_0$  and the ratio  $d/a$ . Interestingly, the stratification effects described in (7) can lead to situations where the region of stratification control extends significantly into the suspension below the sediment front while the front itself remains relatively sharp, in part because of the significant decrease in the diffusivity there because of the stratification.

Restricting our attention here to the steadily falling profiles, we drop the time derivative from Eq. (1). Integrating out a derivative with respect to  $z$  then gives

$$\phi[V(\phi) - V_{\text{sed}}] + D \frac{\partial \phi}{\partial z} + A = 0. \tag{9}$$

Assuming continuously differentiable concentrations (profiles that contradict this assumption are unstable), the boundary conditions at  $z \rightarrow \pm \infty$  on  $\phi$  (with  $\partial \phi / \partial z \rightarrow 0$ ) require<sup>20</sup>  $A = 0$  and  $V_{\text{sed}} = V(\phi_0)$ .

We define  $z_f$  to be the minimum height in the frame falling at  $V_{\text{sed}} = V(\phi_0)$  at which  $\phi = 0$ , with  $\phi(z) = 0$  at all  $z > z_f$  and  $\phi(z) > 0$  for all  $z < z_f$ . The asymptotics of the concentration profile immediately below  $z_f$  vary according to whether the velocity fluctuations and diffusivities there are controlled by cell size or stratification. For diffusivities set by cell size, Eq. (9) becomes

$$\frac{\partial \phi}{\partial z} = \frac{[V(\phi_0) - V_0]}{CV_0} \sqrt{\frac{a\phi}{d^3}} + O(\phi^{3/2}), \tag{10}$$

with

$$\phi \approx \frac{a}{d^3} \left( \frac{V_0 - V(\phi_0)}{2CV_0} \right)^2 (z_f - z)^2, \tag{11}$$

as  $z \rightarrow z_f$  from below ( $\phi = 0$  above). The ratio which must remain smaller than unity for cell-size control is then  $\beta/\beta_{\text{crit}} \approx d[V_0 - V(\phi_0)]/(CBaV_0)$  immediately below  $z_f$ . For diffusivities set by stratification, Eq. (9) becomes

$$\left( - \frac{\partial \phi}{\partial z} \right)^{2/5} = \frac{V_0 - V(\phi_0)}{CB^{3/5} a^{2/5} V_0} \phi^{1/5} + O(\phi^{6/5}), \tag{12}$$

with

$$\phi \approx \frac{1}{4B^3 a^2} \left( \frac{V_0 - V(\phi_0)}{CV_0} \right)^5 (z_f - z)^2, \tag{13}$$

as  $z \rightarrow z_f$  from below. The ratio which must remain larger than unity for stratification control is then  $\beta/\beta_{\text{crit}} \approx \{d[V_0 - V(\phi_0)]/(CBaV_0)\}^{5/2}$  immediately below  $z_f$ . That is, the ratio

$$r_\beta \equiv \frac{d[V_0 - V(\phi_0)]}{CBaV_0} = \frac{6.55}{CB} \phi_0 \frac{d}{a}, \tag{14}$$

determines whether the steadily falling concentration profile immediately below  $z_f$  in this dilute model is determined by diffusivities in Eq. (7) which are controlled by cell size ( $r_\beta < 1$ ) or by stratification of the particle concentration ( $r_\beta > 1$ ).

The first-order steady equation given by Eq. (9) is separable ( $A = 0$ ) and can be readily integrated for dilute hindered settling with  $D$  either set by cell size or by stratification, and those regimes can then be matched to each other at the crossover height between stratification control above and cell-size control below. Alternatively, Eqs. (1), (7), and (8) for steadily falling profiles in this dilute model, subject to the boundary conditions of concentration asymptoting to  $\phi_0$  below and  $\phi \rightarrow 0$  above, can be integrated numerically using a simple shooting method. The resulting solutions are indeed quadratic at very small  $(z_f - z) > 0$ , with coefficients as predicted above. Examples of these profiles are plotted in Fig. 5, indicating some effects of changing  $\phi_0$  and  $d/a$ .

At small  $\phi_0$  and small  $d/a$ , when  $r_\beta$  in Eq. (14) is less than unity, the stratification  $\beta$  is below  $\beta_{\text{crit}}$  everywhere in the steadily falling profile, and the steady solutions to the model equations in the  $V_{\text{sed}}$  frame are a balance between self-sharpening due to hindered settling and the diffusivity controlled by the small cell dimension. As seen in the solution plotted in Fig. 5(a) ( $\phi_0 = 10^{-3}, d/a = 70, r_\beta = 0.917$ ), the self-sharpening effect at these small concentrations, scaling like  $\phi$ , is weak compared to the diffusivity, scaling like  $\sqrt{\phi}$ , and the resulting concentration profile is spread out over an  $O(100d)$  height.

As either  $\phi_0$  or  $d/a$  is increased so that  $r_\beta$  in Eq. (14) becomes larger than unity, the steady solutions in the  $V_{\text{sed}}$  frame have  $\beta$  increasing with increasing  $z$ , and  $\beta > \beta_{\text{crit}}$  in  $z_\beta < z < z_f$  for some  $z_\beta$  where  $\beta = \beta_{\text{crit}}$ . This distance between the crossover height,  $z_\beta$ , and the top of the sediment,  $z_f$ , is found analytically in the dilute model to satisfy  $\frac{2}{3}(r_\beta + 2)\sqrt{r_\beta - 1} = (6.55/C)^{5/2} B^{-3/2} a^{-1} \phi_0^2 (z_f - z_\beta)$ . Examples of such solutions are plotted in Fig. 5(b) ( $\phi_0 = 2 \cdot 10^{-3}, d/a = 70, r_\beta = 1.834$ ) and Fig. 5(c) ( $\phi_0 = 5 \cdot 10^{-3}, d/a = 100, r_\beta = 6.55$ ), with the front profiles sharpening as  $\phi_0$  and  $d/a$  increase. The hindered settling effect is indeed increased with increasing  $\phi_0$ ; but also important to this sharpening in the dilute systems considered in these figures is the sharp reduction of the diffusivities in the region of the front, because of the stratification control of the fluctuations there.

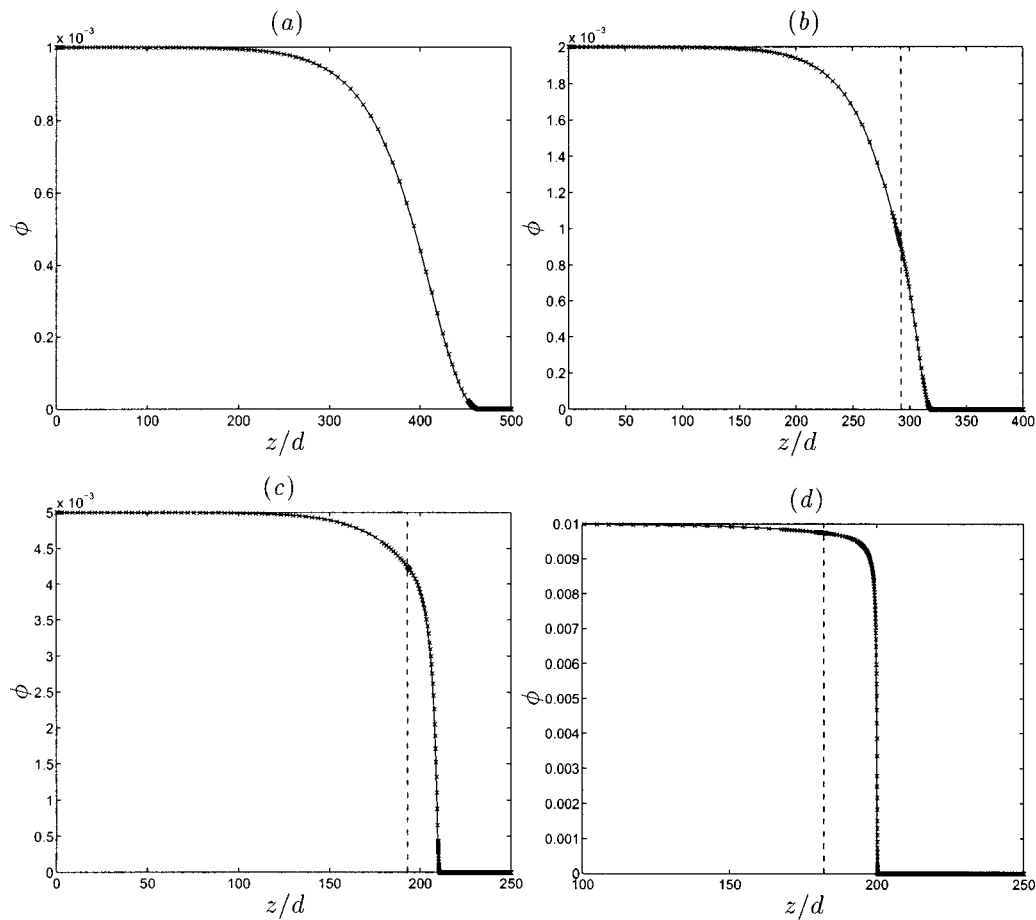


FIG. 5. Steady traveling wave solutions of the dilute sedimentation model (Sec. IV) for the front between particle-laden fluid below, at  $\phi = \phi_0$ , and clear fluid above ( $\phi = 0$ ): (a)  $\phi_0 = 0.1\%$ ,  $d/a = 70$ ; (b)  $\phi_0 = 0.2\%$ ,  $d/a = 70$ ; (c)  $\phi_0 = 0.5\%$ ,  $d/a = 100$ ; (d)  $\phi_0 = 1.0\%$ ,  $d/a = 300$ . The dashed line in (b)–(d) indicates the heights at which  $\beta = \beta_{\text{crit}}$ , with  $\beta < \beta_{\text{crit}}$  below the dashed line (fluctuations and diffusivities controlled by cell size) and  $\beta > \beta_{\text{crit}}$  above (controlled by stratification).

Indeed, the crossover point  $z_\beta$  is below  $z_{90}$ , the point in the steadily falling front where  $\phi = 0.9\phi_0$ , when  $r_\beta > 10$  in the dilute model.

As  $\phi_0$  and  $d/a$  are further increased in this model, the  $z_\beta$  point moves further into the bulk of the sediment, away from the steadily falling front. For instance, Fig. 5(d) shows the steady solution in the  $V_{\text{sed}}$  frame for  $\phi_0 = 0.01$ ,  $d/a = 300$  ( $r_\beta = 39.3$ ), with a much sharper front than the previous figures, with the crossover point  $z_\beta$  separating cell-size control below from stratification control above occurring  $O(20d)$  below the steadily falling front.

Figure 6 indicates the relative importance of the stratification controlling effect, expanding on the sequence of figures discussed above, as a phase diagram in  $\phi_0$  and  $d/a$ . As indicated by the diagram, stratification control of the fluctuations and the diffusivity can extend well below the front itself. Figure 6 also includes a number of symbols indicating some parameters that have been reported in the literature in studies of velocity fluctuations and hydrodynamically induced diffusion.<sup>11,12,24,31–34</sup>

It needs to be emphasized that the model considered in this section and the resulting steadily falling concentration profiles are rough approximations, and the positions of the “phase boundaries” in Fig. 6 are thus only estimates. The

model neglects a number of issues, including the role of collective vs individual diffusive motion, and the possible breakdowns of assumed separations of length scales between the characteristic length of concentration change  $\beta^{-1}$ , the swirl size  $\ell$ , and the discrete particle lengths  $a$  and  $a\phi^{-1/3}$ . Additionally, the model as presented in the present section completely ignores polydispersity effects, which are necessarily present in any physical experiment. Nevertheless, since the purpose of the present work is to emphasize the necessity of extending the functional dependence of  $D$  to vertical concentration gradients, we continue to ignore polydispersity effects here, despite their importance. Also important in many real experiments are effects due to the breakdown of the dilute approximation; before concluding we consider a possible extension of the present model to sedimentation at higher volume fractions.

## V. EXTENSION TO DENSE SEDIMENTATION

The presentation above is built upon a foundational understanding of particle velocity fluctuations in sedimentation at low volume fractions, with emphasis on fluctuations controlled by local stratification of the particle number density. A significant number of experimental measurements of the ve-

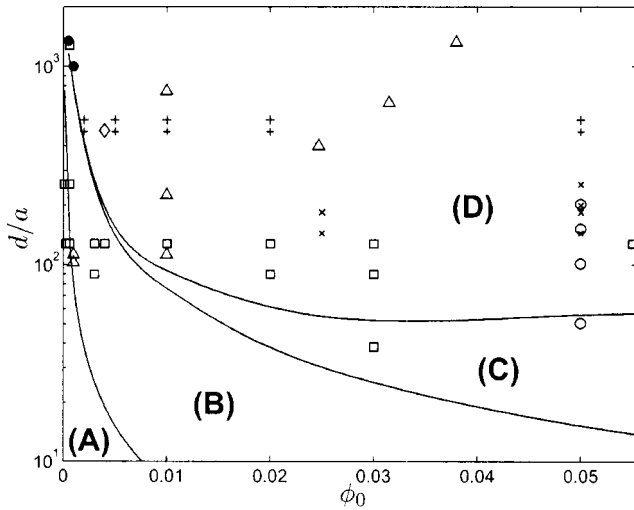


FIG. 6. Phase diagram in the parameters  $\phi_0$  and  $d/a$  indicating selected behaviors of steadily falling fronts in the dilute continuum model (Sec. IV). The different regions identify the extent of stratification control in terms of the small cell dimension,  $d$ , and the relative positions of the top of the front,  $z_f$ ,  $\phi(z_f)=0$ ; the point of the front at 90% bulk concentration,  $z_{90}$ ,  $\phi(z_{90})=0.9\phi_0$ ; and the height at which stratification control begins,  $z_\beta$ , separating cell size control below  $z_\beta$  from stratification control for  $z > z_\beta$ . The solid curves indicate the boundaries between the regions: (A) No stratification control of the diffusivities anywhere in the front,  $r_\beta < 1$  in Eq. (14); (B) stratification control for  $z > z_\beta$ ,  $z_{90} < z_\beta < z_f$ ,  $1 < r_\beta < 10$ ; (C) stratification control extends below the front,  $(z_{90} - 3d) < z_\beta < z_{90}$ ,  $r_\beta > 10$ ,  $\frac{2}{3}(r_\beta + 2)\sqrt{r_\beta - 1} - 24 < 3\phi_0^2(d/a)(6.55/C)^{5/2}B^{-3/2}$ ; (D) stratification control extends further below the front,  $z_\beta < (z_{90} - 3d)$ . The plotted symbols indicate the parameter ranges reported by Ham and Homsy (Ref. 11) ( $\times$ ); Davis and Hassen (Ref. 12) ( $+$ ); Nicolai and Guazzelli (Ref. 32) ( $\circ$ ); Segrè, Herzolzheimer, and Chaiken (Ref. 31) ( $\square$ ); Guazzelli (Ref. 33) ( $\bullet$ ); Lei, Ackerson, and Tong (Ref. 34) ( $\diamond$ ); and Tee *et al.* (Ref. 24) ( $\triangle$ ).

locity fluctuations and diffusivities have been made at higher volume fractions. In particular, the recent work of Segrè *et al.*<sup>35</sup> directly connected measured velocity fluctuations through the full range of volume fractions to previous experiments and hypotheses<sup>31</sup> about dilute systems, the higher volume fraction results being related to dilute behavior in terms of well-known empirical functions of volume fraction for hindered settling, effective viscosity, and the structure factor. While the existing theory of stratification-controlled fluctuations is restricted to dilute systems, we might hypothesize a similar extension to higher volume fractions from the same empirical relationships. Further experimental measurements are necessary to investigate the details of stratification effects in dense sedimentation; in the absence of such knowledge, we consider below a hypothesized extension of the dilute theory. While the details of this dense model certainly remain open to question, we consider it likely that stratification continues to play an essential role in the development and behavior of fluctuations, and therefore the diffusivity should continue to depend on  $\partial\phi/\partial z$  in dense sedimentation.

Using the structure factor  $S(\phi, 0)$  to describe the effects of excluded volume on the number fluctuations, the physical argument that the critical stratification is (up to a constant  $B$ ) that  $\beta$  where the  $\Delta\phi$  due to stratification over a height  $d$  is the same as that expected due to number fluctuations yields

$$\beta_{\text{crit}} \equiv \frac{B}{d} \sqrt{\frac{S(\phi, 0)}{\phi(d/a)^3}}, \quad (15)$$

which differs from Eq. (8) only by the factor  $S(\phi, 0)$ . Continuing the stratification arguments in this setting, the largest surviving swirls in a given stratification  $\beta > \beta_{\text{crit}}$  are at a scale

$$\ell \sim d \left( \frac{\beta}{\beta_{\text{crit}}} \right)^{-2/5} \sim a \phi^{-1/5} [S(\phi, 0)]^{1/5} (\beta a)^{-2/5}. \quad (16)$$

Combining Segrè *et al.* proposal for the role of effective viscosity<sup>35</sup> with the assumption of otherwise Poisson fluctuations corrected by the structure factor up to the scale  $\ell$  then gives

$$\Delta V \sim V_0 \frac{\eta_0}{\eta(\phi)} \left( \frac{\beta}{\beta_{\text{crit}}} \right)^{-1/5} \sqrt{\phi S(\phi, 0) d/a}, \quad (17)$$

giving a diffusivity  $D \sim \ell \Delta V$

$$D = C d V_0 \frac{\eta_0}{\eta(\phi)} \left( \frac{\beta}{\beta_{\text{crit}}} \right)^{-3/5} \sqrt{\phi S(\phi, 0) d/a}, \quad (18)$$

with dimensionless constant  $C$ . When  $\beta < \beta_{\text{crit}}$ , the stratification correction ratio  $\beta/\beta_{\text{crit}}$  in Eqs. (16)–(18) is replaced by unity.

We use the same empirical relationships as Segrè *et al.*: The Richardson–Zaki relationship for hindered settling,<sup>36</sup>  $V(\phi)/V_0 = (1 - \phi)^5$ ; effective viscosities for high shear rate and large Peclet number,<sup>37,38</sup>  $\eta(\phi)/\eta_0 = (1 - \phi/0.71)^{-2}$ ; and  $S(\phi, 0) = [\partial\Pi/\partial\phi]^{-1}$  with the Carnahan–Starling equation of state,<sup>39</sup>  $\Pi(\phi) = (\phi + \phi^2 + \phi^3 - \phi^4)/(1 - \phi)^3$ . Continuing to use the dimensionless constants  $B = 1/2$  and  $C = 1$  completes the definition of the advection-diffusion model in Eq. (1).

Again, we restrict our attention here to the resulting steady-state concentration profiles between  $\phi_0$  bulk concentrations below the front and  $\phi = 0$  clear fluid above. While the first-order Eq. (9) continues to be separable in each  $\beta$  regime, the integrals are not easily found in closed form. Since the  $z \rightarrow z_f$  asymptotics in Sec. IV did not depend on the detailed form of the hindered settling function, only that it was a power series in  $\phi$  at small concentrations, the discussion of dilute asymptotics extends to the dense model considered here, the additional factors of effective viscosity and structure factor appearing only at higher order in  $\phi$ . The ratio

$$r_\beta^{\text{dense}} \equiv \frac{d[V_0 - V(\phi_0)]}{C B a V_0} = \frac{1 - (1 - \phi_0)^5}{C B} \left( \frac{d}{a} \right), \quad (19)$$

determines whether the entire steadily falling front has cell-size controlled diffusivities ( $r_\beta^{\text{dense}} < 1$ ), or whether there is a  $z_\beta < z_f$  where  $\beta = \beta_{\text{crit}}$  and with  $\beta > \beta_{\text{crit}}$  for  $z_\beta < z < z_f$  ( $r_\beta^{\text{dense}} > 1$ ).

A phase diagram in  $(\phi_0, d/a)$  for this dense sedimentation model is shown in Fig. 7. As indicated in the diagram, stratification control of the fluctuations and diffusivities does extend significantly below the front for a wide range of parameters, though the distance decreases at higher volume fractions where the hindered settling effect is stronger. The figure also indicates some of the  $(\phi_0, d/a)$  parameters re-

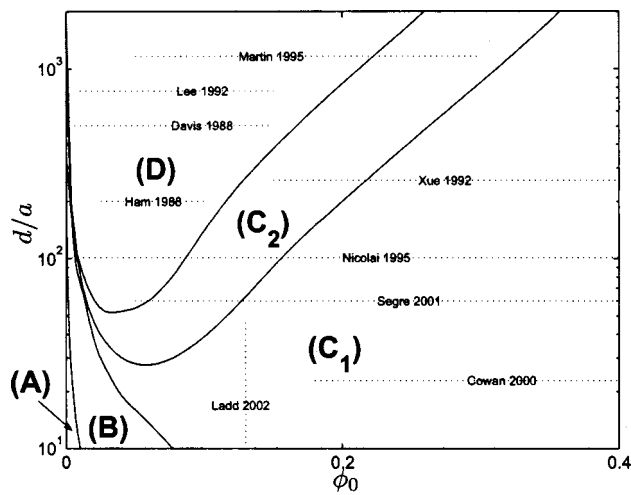


FIG. 7. Phase diagram in the parameters  $\phi_0$  and  $d/a$  indicating selected behaviors of steadily falling fronts in the dense continuum model (Sec. V). The different regions identify the extent of stratification control in terms of the small cell dimension,  $d$ , and the relative positions of the top of the front,  $z_f$ ,  $\phi(z_f)=0$ ; the point of the front at 90% bulk concentration,  $z_{90}$ ,  $\phi(z_{90})=0.9\phi_0$ ; and the height at which stratification control begins,  $z_\beta$ , separating cell size control below  $z_\beta$  from stratification control at all  $z > z_\beta$ . The solid curves indicate the boundaries between the regions: (A) No stratification control of the diffusivities anywhere in the front,  $r_\beta^{\text{dense}} < 1$  in Eq. (19); (B) stratification control for  $z > z_\beta$ ,  $z_{90} < z_\beta < z_f$ ; (C<sub>1</sub>) stratification control extends below the front,  $(z_{90} - 1.5d) < z_\beta < z_{90}$ ; (C<sub>2</sub>) stratification control extends below the front,  $(z_{90} - 3d) < z_\beta < (z_{90} - 1.5d)$ ; (D) stratification control extends further below the front,  $z_\beta < (z_{90} - 3d)$ . Parameter ranges reported experimentally. (Refs. 11–13, 15, 19, 21, 35, 40) and in simulations (Ref. 26) are identified by first author and year.

ported in the literature for the study of velocity fluctuations and hydrodynamically induced diffusion in sedimentation and fluidized beds.<sup>11–13,15,19,21,26,35,40</sup>

## VI. CONCLUDING REMARKS

Dilute-limit “point-particle” interactions between large numbers of monodisperse sedimenting spherical particles were simulated to study the hydrodynamically induced diffusivity of the particle concentration in the vicinity of the falling front between particle-laden fluid below and clarified fluid above. The diffusivities measured from the simulation data fail to satisfy any hypothesized dependence solely on local volume fraction,  $\phi$ . Rather, the diffusivities are roughly approximated by the scaling predicted by stratification control of the correlation length and velocity fluctuations.<sup>24</sup> This model for stratification control of diffusivities, Eq. (7), is combined with Batchelor’s formula for hindered settling<sup>10</sup> to model dilute sedimentation as an advection-diffusion process. A possible extension to higher volume fractions, through considerations analogous to those presented by Segrè *et al.*,<sup>35</sup> is used to model dense sedimentation.

Whether or not a given experiment is influenced by the effects of stratification of the particle concentration, and to what extent, requires a more detailed analysis than that presented here, requiring the investigation of both the time evolution of the profiles from initial conditions and the effects of polydispersity.<sup>41–43</sup> Nevertheless, the results presented here suggest that the wide spread in reported

diffusivities<sup>11–13,15,19,20,23</sup> as functions of  $\phi$  may be a consequence not just of detailed differences in the experimental measurements, but may also be strongly influenced by the stratification control considered here. Meanwhile, the phase diagram for the dense model, Fig. 7, appears to indicate a wide but limited range of conditions under which the stratification effect is relatively small; in these cases, the  $D = D(\phi)$  model is probably not too inaccurate, though the diffusivities at low Reynolds number should then be cell size dependent. Outside of these limited conditions, the particle diffusivity strongly depends on both  $\phi$  and  $\partial\phi/\partial z$ .

## ACKNOWLEDGMENTS

This work was originally presented at the Symposium on Multi-Component and Multiphase Fluid Dynamics, in celebration of Daniel D. Joseph’s pioneering contributions to all kinds of fluid mechanics, at the fourteenth U.S. National Congress of Theoretical and Applied Mechanics. This research was supported by the NSF through the Division of Mathematical Sciences.

- <sup>1</sup>J. Happel and H. Brenner, *Low Reynolds Number Hydrodynamics* (Martinus Nijhoff, The Hague, 1983), paperback ed.
- <sup>2</sup>M. R. Maxey and J. J. Riley, “Equation of motion for a small rigid sphere in a nonuniform flow,” *Phys. Fluids* **26**, 883 (1983).
- <sup>3</sup>R. H. Davis and A. Acrivos, “Sedimentation of noncolloidal particles at low Reynolds numbers,” *Annu. Rev. Fluid Mech.* **17**, 91 (1985).
- <sup>4</sup>E. M. Tory, *Sedimentation of Small Particles in a Viscous Fluid* (Computational Mechanics, Southampton, 1996), Chap. 1.
- <sup>5</sup>R. Bürger and W. L. Wendland, “Sedimentation and suspension flows: Historical perspective and some recent developments,” *J. Eng. Math.* **41**, 101 (2001).
- <sup>6</sup>P. Mazur and W. van Saarloos, “Many-sphere hydrodynamic interactions and mobilities in a suspension,” *Physica A* **115**, 21 (1982).
- <sup>7</sup>J. F. Brady and G. Bossis, “Stokesian dynamics,” *Annu. Rev. Fluid Mech.* **20**, 111 (1988).
- <sup>8</sup>A. J. C. Ladd, “Hydrodynamic transport coefficients of random dispersions of hard spheres,” *J. Chem. Phys.* **93**, 3484 (1990).
- <sup>9</sup>W. O. Kermack, A. G. M’Kendrick, and E. Ponder, “The stability of suspensions. III. The velocities of sedimentation and of cataphoresis of suspensions in a viscous fluid,” *Proc. R. Soc. Edinburgh* **49**, 170 (1929).
- <sup>10</sup>G. K. Batchelor, “Sedimentation in a dilute suspension of spheres,” *J. Fluid Mech.* **52**, 245 (1972).
- <sup>11</sup>J. M. Ham and G. M. Homsy, “Hindered settling and hydrodynamic dispersion in quiescent sedimenting suspensions,” *Int. J. Multiphase Flow* **14**, 533 (1988).
- <sup>12</sup>R. H. Davis and M. A. Hassen, “Spreading of the interface at the top of a slightly polydisperse sedimenting suspension,” *J. Fluid Mech.* **196**, 107 (1988); corrigendum **202**, 598 (1989).
- <sup>13</sup>J. Z. Xue, E. Herbolzheimer, M. A. Rutgers, W. B. Russel, and P. M. Chaikin, “Diffusion, dispersion, and settling of hard-spheres,” *Phys. Rev. Lett.* **69**, 1715 (1992).
- <sup>14</sup>D. L. Koch, “Hydrodynamic diffusion in a suspension of sedimenting point particles with periodic boundary conditions,” *Phys. Fluids* **6**, 2894 (1994).
- <sup>15</sup>H. Nicolai, B. Herzhaft, E. J. Hinch, L. Oger, and E. Guazzelli, “Particle velocity fluctuations and hydrodynamic self-diffusion of sedimenting non-Brownian spheres,” *Phys. Fluids* **7**, 12 (1995).
- <sup>16</sup>R. E. Caflisch and J. H. C. Luke, “Variance in the sedimentation speed of a suspension,” *Phys. Fluids* **28**, 759 (1985).
- <sup>17</sup>E. J. Hinch, in *Disorder and Mixing*, edited by E. Guyon, J.-P. Nadal, and Y. Pomeau (Kluwer Academic, Dordrecht, 1988), Chap. IX, pp. 153–161.
- <sup>18</sup>S. Ramaswamy, “Issues in the statistical mechanics of steady sedimentation,” *Adv. Phys.* **50**, 297 (2001).
- <sup>19</sup>S. Lee, Y. Jang, C. Choi, and T. Lee, “Combined effect of sedimentation velocity fluctuation and self-sharpening on interface broadening,” *Phys. Fluids A* **4**, 2601 (1992).
- <sup>20</sup>J. Martin, N. Rakotomalala, and D. Salin, “Hydrodynamic dispersion

- broadening of a sedimentation front," *Phys. Fluids* **6**, 3215 (1994).
- <sup>21</sup>J. Martin, N. Rakotomalala, and D. Salin, "Hydrodynamic dispersion of noncolloidal suspensions: Measurement from Einstein's argument," *Phys. Rev. Lett.* **74**, 1347 (1995).
- <sup>22</sup>J. Martin, N. Rakotomalala, and D. Salin, "Accurate determination of the sedimentation flux of concentrated suspensions," *Phys. Fluids* **7**, 2510 (1995).
- <sup>23</sup>R. Bürger, F. Concha, and F. M. Tiller, "Applications of the phenomenological theory to several published experimental cases of sedimentation processes," *Chem. Eng. J.* **80**, 105 (2000).
- <sup>24</sup>S.-Y. Tee, P. J. Mucha, L. Cipolletti, S. Manley, M. P. Brenner, P. N. Segrè, and D. A. Weitz, "Nonuniversal velocity fluctuations of sedimenting particles," *Phys. Rev. Lett.* **89**, 054501 (2002).
- <sup>25</sup>J. H. C. Luke, "Decay of velocity fluctuations in a stably stratified suspension," *Phys. Fluids* **12**, 1619 (2000).
- <sup>26</sup>A. J. C. Ladd, "Effects of container walls on the velocity fluctuations of sedimenting spheres," *Phys. Rev. Lett.* **88**, 048301 (2002).
- <sup>27</sup>G. J. Kynch, "A theory of sedimentation," *Trans. Faraday Soc.* **48**, 166 (1952).
- <sup>28</sup>Additional details about the theory of stratification control of velocity fluctuations, summarized in Ref. 24 and again here in Sec. II, will be presented in a future publication, including calculations of the Poisson velocity fluctuations with side walls, a model structure factor calculation with a concentration stratification, direct comparison of velocity fluctuations in simulations with measured stratification, and comparison with experimentally measured velocity fluctuations. Such supporting details are unnecessary for the argument of the present manuscript, wherein the need to include the vertical gradient of concentration as a parameter in the diffusivity has been obtained independently from the simulation results presented in Figs. 1–3.
- <sup>29</sup>M. P. Brenner, "Screening mechanisms in sedimentation," *Phys. Fluids* **11**, 754 (1999).
- <sup>30</sup>E. M. Tory, "Stochastic sedimentation and hydrodynamic diffusion," *Chem. Eng. J.* **80**, 81 (2000).
- <sup>31</sup>P. N. Segrè, E. Herbolzheimer, and P. M. Chaikin, "Long-range correlations in sedimentation," *Phys. Rev. Lett.* **79**, 2574 (1997).
- <sup>32</sup>H. Nicolai and E. Guazzelli, "Effect of the vessel size on the hydrodynamic diffusion of sedimenting spheres," *Phys. Fluids* **7**, 3 (1995).
- <sup>33</sup>E. Guazzelli, "Evolution of particle-velocity correlations in sedimentation," *Phys. Fluids* **13**, 1537 (2001).
- <sup>34</sup>X. Lei, B. J. Ackerson, and P. Tong, "Settling statistics of hard sphere particles," *Phys. Rev. Lett.* **86**, 3300 (2001).
- <sup>35</sup>P. N. Segrè, F. Liu, P. Umbanhowar, and D. A. Weitz, "An effective gravitational temperature for sedimentation," *Nature (London)* **409**, 594 (2001).
- <sup>36</sup>J. F. Richardson and W. N. Zaki, "Sedimentation and fluidization I," *Trans. Inst. Chem. Eng.* **32**, 35 (1954).
- <sup>37</sup>C. G. de Kruif, E. M. F. van Iersel, A. Vrij, and W. B. Russel, "Hard sphere colloidal dispersions: Viscosity as a function of shear rate and volume fraction," *J. Phys. Chem.* **83**, 4717 (1985).
- <sup>38</sup>J. W. Bender and N. J. Wagner, "Reversible shear thickening in monodisperse and bidisperse colloidal dispersions," *J. Rheol.* **40**, 899 (1996).
- <sup>39</sup>W. B. Russel, D. A. Saville, and W. R. Schowalter, *Colloidal Dispersions* (Cambridge University Press, Cambridge, 1989).
- <sup>40</sup>M. L. Cowan, J. H. Page, and D. A. Weitz, "Velocity fluctuations in fluidized suspensions probed by ultrasonic correlation spectroscopy," *Phys. Rev. Lett.* **85**, 453 (2000).
- <sup>41</sup>G. K. Batchelor, "Sedimentation in a dilute polydisperse system of interacting spheres. Part 1. General theory," *J. Fluid Mech.* **119**, 379 (1982).
- <sup>42</sup>G. K. Batchelor and C.-S. Wen, "Sedimentation in a dilute polydisperse system of interacting spheres. Part 2. Numerical results," *J. Fluid Mech.* **124**, 495 (1982).
- <sup>43</sup>R. Bürger, K.-K. Fjelde, K. Höfler, and K. H. Karlsen, "Central difference solutions of the kinematic model of settling of polydisperse suspensions and three-dimensional particle-scale simulations," *J. Eng. Math.* **41**, 167 (2001).